

# Four Switch Buck-Boost Quasi Single-Stage Inverter with Smooth Mode Transition Using Three-Mod Modulation Technique

Ebubekir Keskinçilic  
Department of Electrical Electronics Engineering  
Abdullah Gul University  
Kayseri, Türkiye  
ebubekir.keskinçilic@agu.edu.tr

Burak Tekgun  
Department of Electrical Electronics Engineering  
Abdullah Gul University  
Kayseri, Türkiye  
burak.tekgun@agu.edu.tr

**Abstract**— Quasi-single-stage inverters (QSSI) attract attention due to their simple structure and bidirectional operation capability. However, in the buck-boost DC-DC conversion stage, smooth transition, and efficient conversion cannot be achieved when the output voltage is close to the input voltage with the traditional two-mode control method. This is due to the pulse width ratio limitations, and non-idealities of the active and passive components. In this paper, a comparative analysis of the mode transition techniques in QSSIs is presented using methods available for DC/DC converters. The system efficiency and output voltage signal quality are selected as the performance metrics as they are important performance parameters in many applications. A 2kW QSSI is controlled using single-mode, two-mode, and three-mode modulation techniques. Simulation and experimental studies are conducted for validation. Based on these studies, it is concluded that the single-mode modulation technique performed the best in eliminating dead zone effects and reducing total harmonic distortion (THD), whereas the two-mode modulation technique achieved the highest system efficiency. The three-mode modulation has superior performance on dead zone elimination compared to the two-mode modulation and better system efficiency than the single-mode modulation method. Experimental results indicate that the three-mode modulation achieved an efficiency of 91.12% with a THD of 3.73%.

**Keywords**— Quasi-single-stage inverter, four-switch buck-boost converter, dead zone elimination.

## I. INTRODUCTION

Global energy consumption increases by about 50% each decade. In recent years, the demand for sustainable, green, and efficient energy conversion has grown as a result of the rising energy needs. According to a 2020 report by the IEA, fossil-based energy makes up around 70% of total electricity consumption, amounting to approximately 25,000 TWh [1]. Among the converters designed for energy conversion, there is an ongoing effort to improve efficiency while reducing size and cost. Certain power converters necessitate two types of conversion processes: DC-DC and DC-AC. These converters are commonly employed in applications such as renewable energy, power supplies, and electric vehicles, where adjustable AC output is required.

In a typical two-stage power inverter, a boost converter steps up the voltage in the first stage, and an inverter is used to generate the AC voltage in the second [2]–[4]. However, these inverters have drawbacks such as complex control structures, losses associated with the active and passive components, increased costs, and larger sizes due to their two-stage power conversion mechanisms. Other inverters like the flyback [5], the Z-source [6], and H6 and H8 [7] inverters address the issue of leakage current. However, they encounter

challenges such as complex transfer functions, only supporting operation at unity power factor, and additional power switching drawbacks, respectively.

To address the limitations of the aforementioned inverters, quasi-single-stage (QSS) inverters have been proposed. These inverters offer single-stage power processing with straightforward PWM control, along with a reliable and highly efficient power process, all while eliminating the need for a DC-link filter [8]. In [9], proposed Four-Switch Buck-Boost (FSBB) inverter combines a buck boost converter, which produces a rectified sinus waveform, using a single phase inverter. However, despite its simplicity, this converter faces challenges in managing light load scenarios and regulating reactive power flow. It also struggles with discharging the output capacitor to control the voltage in the negative direction, resulting in efficiency concerns due to the operation of four active switches within one switching cycle [10].

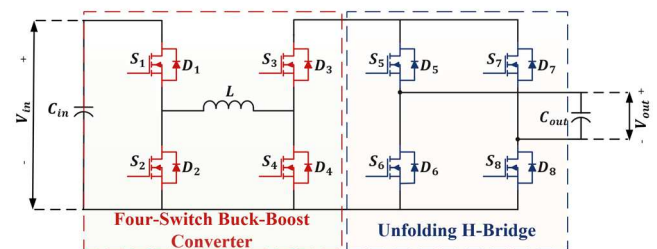


Fig. 1. The four-switch buck-boost inverter circuit

The DC-DC section of the FSBB inverter switches between buck and boost modes to produce a rectified sinus wave for transition to the unfolding circuit [11]. However, when performing with these modes, termed two-mode control, when the voltage input matches the output voltage, a continuous transition between states is not achieved. Methods proposed in [12] address this for low-voltage converters, yet issues persist due to duty cycle constraints and increased voltage ripple, as discussed in [13]. While [14] proposes a control method to mitigate this, efficiency is compromised. These challenges, known as the "dead zone," stem from non-ideal conditions and component disturbances, leading to poor regulation and discontinuity around the equilibrium voltage [15].

In [16], the converter works only in buck-boost mode to prevent transition issues and eliminate disruptions from the operational dead zone. While this prevents problems like subharmonics and output voltage ripple, four switches operating continuously in buck-boost mode significantly reduces power conversion efficiency. The "Dead Zone Avoidance and Minimization (DZAM)" control [17], utilizes

nonlinear state machine models ensuring fast and precise converter regulation while addressing problems such as subharmonics and increased output voltage ripple.

The approach used in [18] includes overlapping the buck and boost states and adding a hysteresis band and an extra buck-boost mode between the two modes, keeping the duty cycle in both states. In [19], an interleaved four-phase method is employed to minimize output voltage distortions and ensure a smooth transition between modes, utilizing a 90° phase shift. In [20], a technique is introduced that employs both step-down and step-up processes during transitions by designating particular duty ratios to each. In [21], control is carried out with the model predictive detection of the modes without any measurements instead of using separate control loops and modulators for the switching states. The buck-boost mode utilized in three-mode techniques removes discontinuities in the transition area by directly implementing the buck-boost mode within the dead zone region.

While many methods have been widely accepted in the literature, particularly focusing on avoiding dead zones for DC-DC applications, research regarding DC-AC applications remains limited. Given that the AC output signal encounters discontinuity every quarter period as the voltage goes from zero to its peak and comes to zero again, it is more affected compared to DC systems. Therefore, in this paper exploring and applying current methods to compare the performance of different mode transition techniques in DC-AC conversion from a fresh perspective is targeted. The primary motivation and state-of-the-art goal of the study is to investigate the dead zone issue by operating the converter in inverter mode. The single, two, and three-mode modulation techniques regarding high-efficiency operation, THD performances, and dead zone elimination capability are investigated and compared. The paper is structured as follows: Section II introduces the circuit analysis and operational principles of the FSBB inverter. Section III elaborates on the origins of the dead zone and explores methods to mitigate it. Section IV presents simulation and experimental results. Finally, Section V summarizes the findings and draws conclusions.

## II. OPERATING PRINCIPLES OF THE FOUR-SWITCH BUCK-BOOST INVERTER

The inverter system shown in Fig. 1 consists of an FSBB DC-DC converter paired with a single-phase unfolding inverter. This type of inverter is classified as a QSS converter, capable of both buck and boost power processing with a single simple circuit design. Compared to single- and two-stage converters, this quasi-single-stage structure excels because it has a larger output voltage and current range, less stress on a single active element's voltage, and reduced input and output harmonics. Moreover, compared to conventional two-stage converters, the FSBB inverter has the benefits of increased efficiency, less component needs, and inherent four-quadrant operation.

$V_{in}$  and  $V_{out}$  are input and output voltages, respectively as shown in Fig. 1. The DC-DC stage of the selected inverter consist of MOSFET's switching at high frequency,  $S_1 \sim S_4$  with four corresponding body diodes,  $D_1 \sim D_4$ , to perform buck and boost modes with an inductor  $L$ . Filtering capacitors are positioned at input and output, respectively. The switches operate synchronously within one stage. Whilst the switches are turned off, the corresponding antiparallel diodes provide a current path [22]. The inverter is linked to the FSBB in order

to produce the DC-AC conversion. Its function is to flip the polarity of an input signal to produce a sine wave. The unfolding inverter is an H-Bridge inverter that works at twice the AC signal frequency when the output voltage crosses zero. As the single-phase inverter is only responsible for inverting the rectified sinus waveform taken from the DC-DC conversion stage, the inverter's operation and the choice of passive components are specified.

The FSBB converter has four switches: the switches on the left side are referred to as buck switches, while those on the right side are known as boost switches. The FSBB can operate in three conventional modes namely buck mode, boost mode, as well as the buck-boost mode in one stage. The mode selection depends ratio of the input and output voltages. Both leg switches operate in a complementary conduction to prevent shoot-through. In an ideal scenario, where the inductor's parasitic resistance, power switches, and active and passive component losses are ignored, the gain of the converter is governed by the voltage-second balance principle of the inductor. The duty cycle of the  $S_1$  switch is denoted by  $d_1$ , and the duty cycle of the  $S_4$  switch is denoted by a  $d_2$ . The voltage gain of the FSBB represented as  $M$ , is expressed as follows

$$M = \frac{V_{out}}{V_{in}} = \frac{d_1}{1-d_2} \quad (1)$$

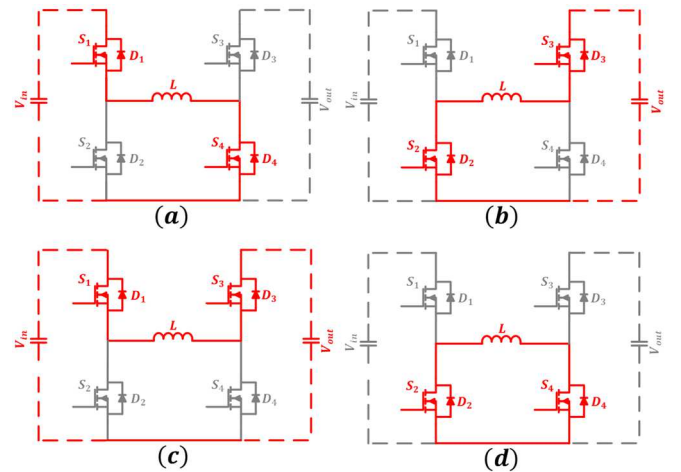


Fig. 2. Four switching modes of the FSBB. (a) Boost mode, (b) Buck mode, (c) Bypassing mode, (d) Freewheel mode

The converter output voltage is adjusted based on the input voltage by modifying  $d_1$  and  $d_2$ , which are the duty cycle ratios for the buck and boost switches, respectively. This allows for independent control over the voltage gain. As indicated by (1), the desired voltage gain can be achieved with various combinations of  $d_1$  and  $d_2$  respectively. Consequently, the switching states, along with the current paths for the states are highlighted by the color red presented in Fig 2.

FSBB converter has four potential switching states whilst buck, boost and buck-boost operations can be performed by creating binary combinations with them. The traditional operating modes shown in Fig. 2, along with their active switching states and duty cycles are detailed in Table 1.

TABLE I. SWITCHING STATES

Modes	$S_1$	$S_2$	$S_3$	$S_4$	Gain
<b>Buck Mode</b>	Switching	Switching	On	Off	$d_1$
<b>Boost Mode</b>	On	Off	Switching	Switching	$\frac{1}{1-d_2}$
<b>Buck-Boost Mode</b>	Switching	Switching	Switching	Switching	$\frac{d_1}{1-d_2}$

III. DEAD ZONE MITIGATION TECHNIQUES

The duty cycle of every switch in the FSBB topology must be configured in accordance with the converter's operating mode. Under ideal circumstances, there would be no time delay or gap when transitioning from buck/boost to boost/buck mode variations, except for unavoidable non-idealities, such as erratic switching noises, disruptions in circuit layout issues, and passive and active elements. However, in practical scenarios, the transition between the buck and boost states might lead to uncontrollability, even because of the discontinuity brought on by gating circuits and the switching time delay of switches [23]. This discontinuity, due to the switching delay during mode transitions, can lead to increased output voltage ripple when duty ratios near 0-10% and 90-100%. By redefining (1) let's introduce an additional parameter,  $\delta$ , that denotes the gradient of a the line that defines the functional relationship between the buck and boost modes duties required for the output-to-input relation.

$$\delta = \frac{1}{M} = \frac{1-d_2}{d_1} \tag{2}$$

According to (2), it can be seen that the slope  $\delta$  is generated by separately adjusting the duty cycles of the boost and buck switches. If the relationship between  $d_1$  and  $d_2$  is to be shown graphically,  $d_1$  can be placed as the abscissa and  $1-d_2$  as the ordinate, as in Fig. 3 for both ideal and actual operation.

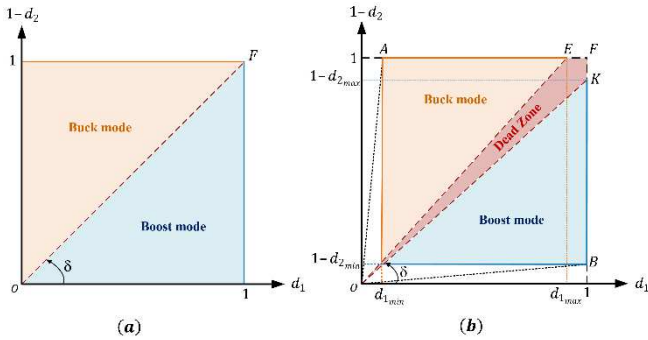


Fig. 3. Two-mode operation with (a) Ideal and (b) Real operating conditions

In Fig. 3(a), the slope and voltage gain of the dashed red line are both 1. When the converter operates in buck mode, the parameter  $1-d_2$  or  $d_1$  is set to 1, while in boost mode,  $d_1$  or  $1-d_2$  is set to 1. This approach, known as the traditional two-mode control [19], is considered ideal under perfect conditions. However, as illustrated in Fig. 3(b), real-world limitations affect buck and boost operations. The buck states are represented by the AOE area highlighted in orange color, the boost state by the KOB area highlighted in blue color, and the inactive zone between two states is indicated by the OEFK area highlighted with the red non-uniform rectangle. The area between OE and OK are critical for operation, as they are

necessary to achieve the desired voltage gain when the output voltage is near the input voltage [24].

There are various methods in literature to avoid dead zone effect and with respect to active power losses, switching, and complexity of the control circuit, each of these approaches has advantages and disadvantages. This paper examines single and three mode modulation methods for avoiding dead zones based on their voltage ripple and efficiency. Using a full buck-boost operation is the most straightforward way to prevent the dead zone during operation. This technique is called "single-mode modulation," which denotes that the FSBB converter operates in the single mode for supplying the full voltage conversion rate while utilizing all switches at once as in Fig. 4.

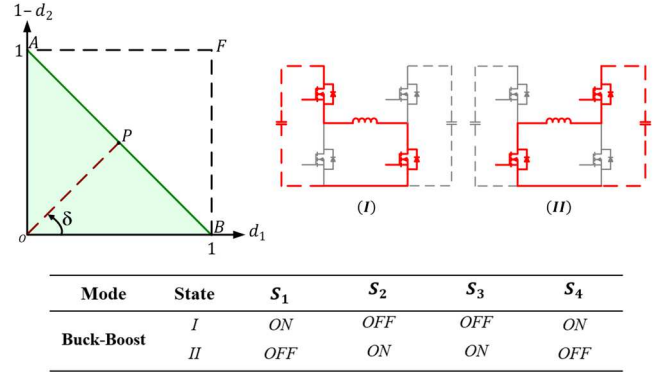


Fig. 4. Single-mode operation scheme

Hence, this mode avoids discontinuous voltage conversion across the whole voltage range. Therefore the duty ratio  $D$  varies between zero and one. By removing the dead zone, one also removes the possibility of any further voltage fluctuation after the level of input-output voltage equivalence is reached. Nevertheless, this modulation technique has been analyzed in [25], for low voltage, the system attains a maximum efficiency of 72%. While the output voltage rises, the efficiency of the system degrades. As all the switches are switching for all operating ranges, switching losses lead to a decrease in converter efficiency.

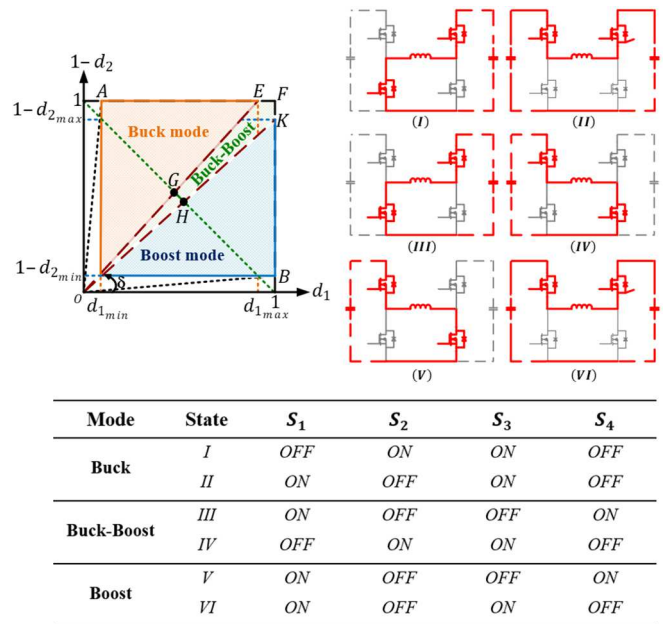


Fig. 5. Three-mode operation scheme

Although the single modulation technique is successful in eliminating dead zones, a technique that eliminates discontinuity, has low power loss, and low control complexity can be obtained to address its disadvantages. Called three-mode modulation [26], this technique pushes the high efficiency of traditional two-mode modulation to the limits and then creates an operating mode that combines it with the dead zone elimination capabilities of the buck-boost mode. As seen in Fig. 5, the buck mode operates up to the limit value, then the buck-boost mode operates in the dead zone, and finally, the boost mode completes the entire cycle.

The buck-boost operation during the mode transitions is a downside of the three-mode modulation approach. To operate in the boost or buck mode, solely two MOSFETs need to be operating at each cycle. However, in the buck-boost mode, all the MOSFETs are switching and the losses are switching dramatically increase [27].

The efficiency of the system is calculated by considering the losses arising from passive components, active elements, and semiconductors should be taken into account separately and subtracted from the total. Passive components' losses can be obtained by modeling the non-idealities of the capacitor and inductor. Although the losses occurring on the semiconductor side may vary depending on the circuit used, they generally consist of diode and switch losses. These are further detailed as switching and conduction losses and separately calculated. Diode losses also take place during the switching. Similarly, diode losses are also separately calculated as reverse recovery and conduction losses. The calculation methods used here apply to both MOSFETs and diodes in the analyses. The calculation methods used in [28] are applied to both MOSFETs and diodes in system efficiency calculation analyses.

#### IV. SIMULATION AND EXPERIMENTAL RESULTS

The QSSI is built and tested in both a lab setting and a computer environment to verify, compare, and prove the efficacy of the two mentioned methods over the single-mode and two-mode modulation methods. The inverter design relies on active and passive circuit components, including the input and output capacitors ( $C_{in}$  and  $C_{out}$ ), the inductor ( $L$ ), and the semiconductor switching devices ( $S_n$ ). "Selecting the values for these components is complex, involving numerous criteria. The inductor design depends on factors such as maximum power, maximum current, inductance, voltage exposure, and switching frequency. When choosing input and output capacitances, the worst-case scenario should be accounted for each component. For selecting MOSFETs, it's essential to know parameters like the on-state resistance, maximum drain-source voltage, maximum ambient temperature, and maximum junction temperature. Considering all performance and operational limitations, the chosen components are a 40  $\mu$ H inductor, 4  $\mu$ F capacitors for both input and output, and SiC power MOSFETs designated C3M0065090J. The 2-kW inverter system features a 200 VDC input and 220 VRMS output, and both simulation and real-time applications use the same parameters, including a 100 kHz switching frequency, to compare the dead zone techniques. To ensure a fair comparison of all modes same conditions are applied consistently to both the experimental setup and the simulations. Fig. 6 illustrates the model built in the PSIM platform while Fig. 7 shows the prototype of the FSBB inverter system used for experimentation.

The test setup, measurement, and power supply equipment include the following components: 1. The prototyped QSSI. 2. Texas Instruments TMS320F28379D LAUNCHPAD for circuit control and communications. 3. AMETEK SGX series DC power supply to provide input DC power 4. Tektronix A622 current probes are used to measure the currents. 5. Pintek DP25 differential voltage probes for output voltage measurements. 6. Resistive load bank with adjustable settings to achieve the desired loading, and 7. Tektronix MDO3000 scope is used to observe and acquire the resulting waveforms.

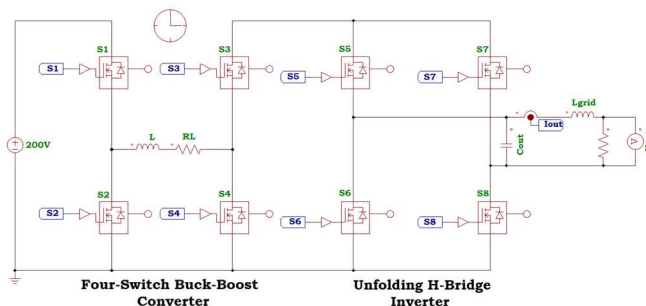


Fig. 6. Simulation circuit of the FSBB inverter

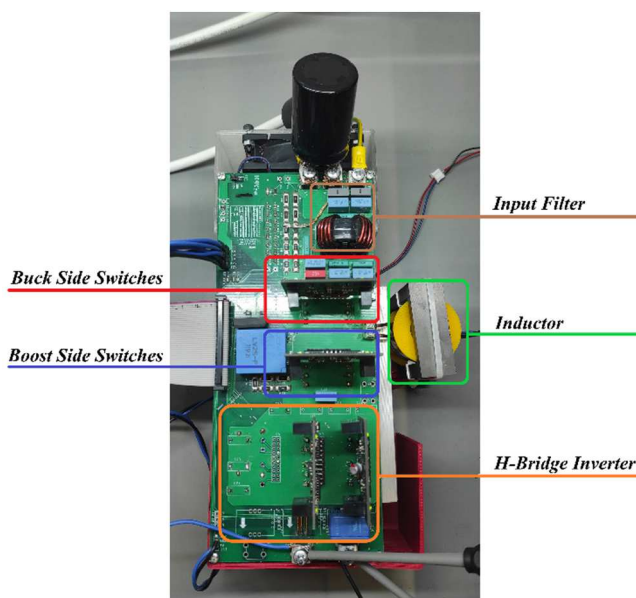


Fig. 7. Experimental setup of the FSBB inverter

The QSSI operates in an open-loop manner in all cases, meaning there is no feedback control system to regulate the output voltage or produce a pure 50 Hz sine wave. Initially, the traditional two-mode operation is used: if the output produces less than 200 V, the inverter functions solely as a buck converter; output exceeds 200 V, the inverter operates exclusively as a boost converter. On the other hand, due to inherent limitations on the duty cycle, the inverter struggles to operate as desired neither in buck nor in boost modes when producing voltage around 200 V. When the inverter generates a sine wave, and the output voltage gets close to 200 V the duty cycle of the buck converter reaches the maximum level of 90%. From this operating condition the mode changes to the boost mode where the minimum duty cycle is 10%. During this commutation period, a discontinuity occurs and the output signal becomes distorted. In contrast, as expected, when the inverter operation mode is selected as single mode, it solely operates as a buck-boost converter, and the resulting waveforms are free of distortions. Finally, when the operating

mode is the three-mode one, waveforms become smoother during the mode commutation. The process begins in buck mode and shifts to buck-boost one when the voltage levels of the input and output are close. During this phase, despite some slight ripple, the operation continues down to the lower limit of the boost mode after the mode transition is complete. Compared to single-mode control, the lossy buck-boost operation is limited, enabling the converter to be controllable within the dead zone, resulting in smoother transitions between modes.

Fig. 8, 9, and 10 show the zoomed-in voltage behavior in the dead zone obtained when the output voltage is desired to be sinusoidal from experimental tests for the single, two, and three mode modulation techniques, respectively. After examining the operating modes of the inverter, comparisons of the inverter's performance parameters regarding efficiency and THD are listed in Tables 2 and 3, respectively, based on simulation and experimental results.

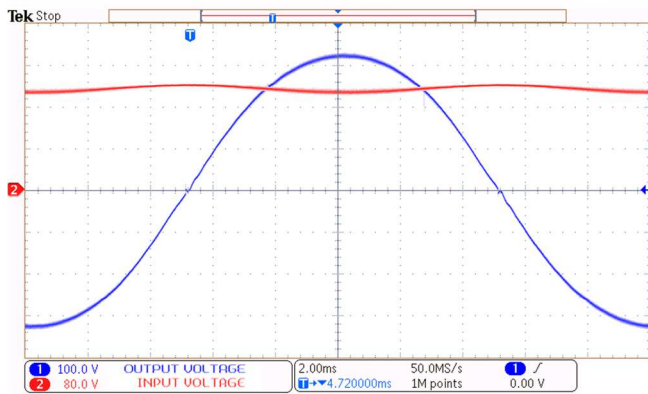


Fig. 8. The output and input voltage of single-mode modulation

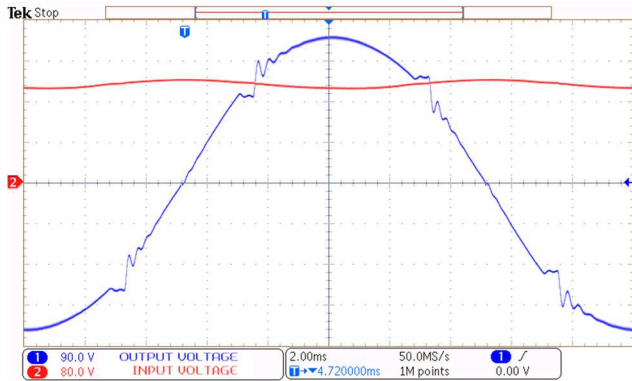


Fig. 9. The output and input voltage of three-mode modulation

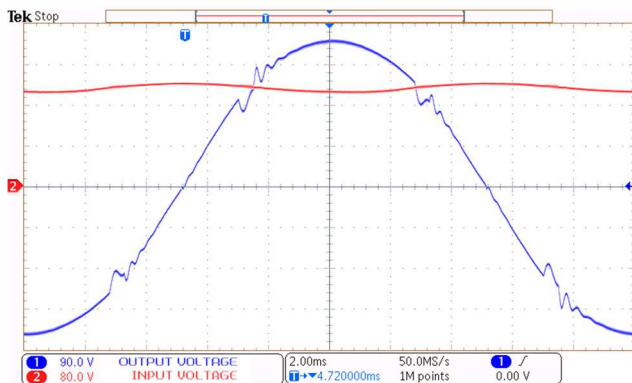


Fig. 10. The output and input voltage of three-mode modulation

TABLE II. SUMMARY OF THE SIMULATION RESULTS

Modulation Technique	Efficiency at full-load	THD at full-load	Elimination of the Dead Zone
Single-Mode	91.09%	0.29%	Yes
Traditional Two-Mode	93.05%	1.64%	No
Three-Mode	92.64%	0.63%	Yes

TABLE III. SUMMARY OF THE EXPERIMENTAL RESULTS

Modulation Technique	Efficiency at full-load	THD at full-load	Elimination of the Dead Zone
Single-Mode	87.81%	3.46%	Yes
Traditional Two-Mode	92.44%	4.62%	No
Three-Mode	91.12%	3.73%	Yes

The experimental and simulation results are proportionally similar; however, due to environmental effects and other non-ideal conditions, the simulation results naturally show higher efficiency and lower distortion across all modes. Therefore, it may be reasonable to make an interpretation based only on experiments.

Single-mode modulation achieves a pure sinusoidal waveform, meaning the dead zone is completely eliminated, but its THD suffers by 3.46% due to dominant third harmonics, and consequently, its efficiency falls below 88% at full load. In traditional two-mode modulation, a significant THD value exceeding 4% is noticeable. Despite achieving good performance with an efficiency of 92.44%, the dead zone occurring when the mode transitions leads to distortions in the output waveforms. However, the three-mode performs better than the mentioned methods by reducing the dead zone and ensuring smoother transitions. The ripple and efficiency issues are reduced but still persist due to the parasitic effects.

## V. CONCLUSION

This article investigates a four-switch buck-boost quasi-single-stage inverter's dead zone issues, focusing on its efficiency and output voltage distortion. Unlike other studies, this research provides a different perspective by examining the dead zone that occurs in FSBB-type converters not only in terms of DC-DC conversion performance but also in terms of inverter operation. This perspective introduces a novel examination approach to the literature by analyzing the converter within the framework of DC-AC operations. It is aimed to identify the root cause of the dead zone during the commutation between the step-down and step-up operations and to determine an effective modulation scheme to eliminate it. Two different dead zone elimination methods with traditional two-mode control are compared to mitigate the dead zone and are thoroughly examined by outlining their operation schemes. The real-time experimental and simulation results were in a similar direction, the three-mode modulation emerged as the superior method among the single and traditional two-mode modulation techniques. According to the results for three-mode modulation at full load scenario, it had 92.64% efficiency and 0.63% THD value for simulation, and 91.12% efficiency and 3.73% THD value in real-time application. In terms of both simulation and experimental results, three-mode modulation offers superior values in terms of efficiency to single-mode modulation and THD than two-mode modulation. Future work will include the effect of the

frequency variation on the efficiency and the electromagnetic interference performance.

## REFERENCES

- [1] IEA World electricity consumption, "World electricity consumption." <https://www.iea.org/fuels-and-technologies/electricity#data-browser> (accessed Apr. 15, 2023).
- [2] T. Yao, Y. Guan, F. Li, Y. Wang, W. Wang, and D. Xu, "A Novel AC/DC Converter Based on Stacked Boost Circuit and Dual-Mode LLC Circuit," *IEEE Trans. Ind. Appl.*, vol. 56, no. 6, pp. 6576–6585, 2020, doi: 10.1109/TIA.2020.3015793.
- [3] C. Wu, J. Chen, X. Chen, and Y. Wang, "Second Harmonic Current Reduction for Two-Stage Single-Phase Rectifier With LLC Converter Based on Charge Control With Nonlinear Feedforward," *IEEE Trans. Power Electron.*, vol. 39, no. 12, pp. 15409–15413, 2024, doi: 10.1109/TPEL.2024.3439366.
- [4] J. A. Solsona, S. G. Jorge, C. A. Busada, and F. A. Mengatto, "Exact Linearization Control of a Two-Stage DC–AC Converter With a Power Pulsating Buffer," *IEEE Trans. Power Electron.*, vol. 39, no. 12, pp. 15870–15879, 2024, doi: 10.1109/TPEL.2024.3445254.
- [5] A. Sarkar, N. Deshmukh, and S. Anand, "Modified PWM Scheme to Reduce Reverse Conduction Loss in GaN-Based Independently Controlled Multiple Output Flyback Converter," *IEEE Trans. Power Electron.*, vol. 37, no. 11, pp. 12968–12972, 2022, doi: 10.1109/TPEL.2022.3182058.
- [6] S. M. J. Mousavi, D. Zargariashar, E. Babaei, and H. F. Ahmed, "A Single-Phase Z-Source AC–AC Converter With Continuous Input Current and Without Commutation Issue," *IEEE Trans. Ind. Electron.*, vol. 71, no. 11, pp. 14002–14010, 2024, doi: 10.1109/TIE.2024.3357889.
- [7] U. A. Khan, A. A. Khan, F. Akbar, and J. W. Park, "Single-Stage Single-Phase H6 and H8 Non-Isolated Buck-Boost Photovoltaic Inverters," *IEEE J. Emerg. Sel. Top. Power Electron.*, vol. 10, no. 4, pp. 4865–4878, 2022, doi: 10.1109/JESTPE.2022.3153840.
- [8] F. Peng, G. Zhou, N. Xu, and S. Gao, "Zero Leakage Current Single-Phase Quasi-Single-Stage Transformerless PV Inverter With Unipolar SPWM," *IEEE Trans. Power Electron.*, vol. 37, no. 11, pp. 13755–13766, 2022, doi: 10.1109/TPEL.2022.3180287.
- [9] M. Çelebi and I. Alan, "A novel approach for a sinusoidal output inverter A novel approach for a sinusoidal output inverter," *Electr. Eng.*, vol. 92, no. 7–8, pp. 239–244, 2010, doi: 10.1007/s00202-010-0181-3.
- [10] B. Tekgun, D. Tekgun, I. Alan, and M. Badawy, "Design and Control of a Single Phase DC/Rectified AC/AC Inverter for low THD Applications," 7th Int. IEEE Conf. Renew. Energy Res. Appl. ICRERA 2018, vol. 5, pp. 424–430, 2018, doi: 10.1109/ICRERA.2018.8566841.
- [11] C. Restrepo, J. Calvente, A. Romero, E. Vidal-Idiarte, and R. Giral, "Current-Mode Control of a Coupled-Inductor Buck–Boost DC–DC Switching Converter," *IEEE Trans. Power Electron.*, vol. 27, no. 5, pp. 2536–2549, 2012, doi: 10.1109/TPEL.2011.2172226.
- [12] A. Chakraborty, A. Khaligh, A. Emadi, and A. Pfaelzer, "Digital Combination of Buck and Boost Converters to Control a Positive Buck-Boost Converter," 2006 37th IEEE Power Electron. Spec. Conf., pp. 1–6, 2006.
- [13] R. Paul and D. Maksimovic, "Smooth transition and ripple reduction in 4-switch non-inverting buck-boost power converter for WCDMA RF power amplifier," *Proc. - IEEE Int. Symp. Circuits Syst.*, pp. 3266–3269, 2008, doi: 10.1109/ISCAS.2008.4542155.
- [14] R. Paul and D. Maksimovic, "Analysis of PWM nonlinearity in non-inverting buck-boost power converters," *PESC Rec. - IEEE Annu. Power Electron. Spec. Conf.*, vol. 3, pp. 3741–3747, 2008, doi: 10.1109/PESC.2008.4592538.
- [15] G. Zhang, J. Yuan, S. S. Yu, N. Zhang, Y. Wang, and Y. Zhang, "Advanced four-mode-modulation-based four-switch non-inverting buck–boost converter with extra operation zone," *IET Power Electron.*, vol. 13, no. 10, pp. 2049–2059, 2020, doi: 10.1049/iet-pel.2019.1540.
- [16] R. Lin and R. Wang, "Non-inverting Buck-Boost Power-Factor-Correction Converter with Wide Input-Voltage-Range Applications," vol. 4, pp. 599–604, 2010.
- [17] D. C. Jones and R. W. Erickson, "A nonlinear state machine for dead zone avoidance and mitigation in a synchronous noninverting buck-boost converter," *IEEE Trans. Power Electron.*, vol. 28, no. 1, pp. 467–480, 2013, doi: 10.1109/TPEL.2012.2198924.
- [18] C. Restrepo, T. Konjedic, J. Calvente, and R. Giral, "Hysteretic transition method for avoiding the dead-zone effect and subharmonics in a noninverting buck-boost converter," *IEEE Trans. Power Electron.*, vol. 30, no. 6, pp. 3418–3430, 2015, doi: 10.1109/TPEL.2014.2333736.
- [19] Y. He, W. Chen, J. Deng, and M. Xu, "A Four-Phase Interleaved Four-Switch Buck-Boost Converter with Smooth Mode Transition Strategy for Fuel Cell System," *Proc. - 2021 IEEE Sustain. Power Energy Conf. Energy Transit. Carbon Neutrality, ISPEC 2021*, pp. 3175–3181, 2021, doi: 10.1109/iSPEC53008.2021.9735634.
- [20] L. Callegaro, M. Ciobotaru, D. J. Pagano, E. Turano, and J. E. Fletcher, "A Simple Smooth Transition Technique for the Noninverting Buck-Boost Converter," *IEEE Trans. Power Electron.*, vol. 33, no. 6, pp. 4906–4915, 2018, doi: 10.1109/TPEL.2017.2731974.
- [21] X. Li, Y. Liu, and Y. Xue, "Four-Switch Buck-Boost Converter Based on Model Predictive Control with Smooth Mode Transition Capability," *IEEE Trans. Ind. Electron.*, vol. 68, no. 10, pp. 9058–9069, 2021, doi: 10.1109/TIE.2020.3028809.
- [22] R. W. Erickson and D. Maksimovic, *Fundamentals of Power Electronics*. Kluwer Academic, 2001.
- [23] G. Kumawat, V. Shah, and S. Payami, "A Universal-Input On-Board Charger Integrated Power Converter for Switched Reluctance Motor Drive Based EV Application," *IEEE Trans. Ind. Appl.*, vol. 60, no. 4, pp. 6458–6468, 2024, doi: 10.1109/TIA.2024.3397952.
- [24] N. Zhang, G. Zhang, and K. W. See, "Systematic Derivation of Dead-Zone Elimination Strategies for the Noninverting Synchronous Buck-Boost Converter," *IEEE Trans. Power Electron.*, vol. 33, no. 4, pp. 3497–3508, 2018, doi: 10.1109/TPEL.2017.2704597.
- [25] B. Hwang, B. Sheen, J. Chen, Y. Hwang, and C. Yu, "A Low-Voltage Positive Buck-Boost Converter Using Average-Current-Controlled Techniques," pp. 23–26, 2012.
- [26] Y. J. Lee, A. Khaligh, A. Chakraborty, and A. Emadi, "Digital Combination of Buck and Boost Converters to Control a Positive Buck-Boost Converter and Improve the Output Transients," *IEEE Trans. Power Electron.*, vol. 24, no. 5, pp. 1267–1279, 2009, doi: 10.1109/TPEL.2009.2014066.
- [27] Q. Ullah, X. Wu, and U. Saleem, "Current Controlled Robust Four-Switch Buck-Boost DC-DC Converter," 2021 Int. Conf. Comput. Electron. Electr. Eng. ICE Cube 2021 - Proc., pp. 1–6, 2021, doi: 10.1109/ICECube53880.2021.9628275.
- [28] B. Tekgun, D. Tekgun, and I. Alan, "A multi-functional quasi-single stage bi-directional charger topology for electric vehicles," *Ain Shams Eng. J.*, vol. 15, no. 3, p. 102471, 2024.